Pergamon

0306-4522(95)00361-4

Neuroscience Vol. 70, No. 2, pp. 597–612, 1996
Elsevier Science Ltd

0306-4522/96 $15.00 + 0.00

X-IRRADIATION-INDUCED CHANGES IN THE DIFFUSION PARAMETERS OF THE DEVELOPING RAT BRAIN

E. SYKOVÁ,*† J. SVOBODA,† Z. ŠIMONOVÁ,† A. LEHMENKÜHLER‡ and H. LASSMANN§

†Laboratory of Cellular Neurophysiology, Institute of Experimental Medicine, Academy of Sciences of the Czech Republic, Vídeňská 1083, 142 20 Prague 4, Czech Republic
‡Institute of Physiology, University of Münster, Robert-Koch-Str. 27a, 48149 Münster, Germany
§Research Unit for Experimental Neuropathology, Austrian Academy of Sciences, Schwarzspanierstr. 17, 1090 Vienna, Austria

Abstract—Three diffusion parameters of brain tissue, extracellular space volume fraction (α), tortuosity (λ) and non-specific uptake (k') of tetramethylammonium were studied in the somatosensory neocortex and subcortical white matter of the rat during postnatal development (postnatal days 2–21) after X-irradiation at postnatal days 0–1. The diffusion parameters were determined from extracellular concentration–time profiles of tetramethylammonium. The tetramethylammonium concentration was measured *in vivo* with ion-selective microelectrodes positioned 130–200 μm from an iontophoretic source. X-irradiation with a single dose of 40 Gy resulted in typical early morphological changes in the tissue, namely cell death, DNA fragmentation, extensive neuronal loss, blood–brain barrier damage, activated macrophages, astrogliosis, increase in extracellular fibronectin and concomitant changes in all three diffusion parameters. The changes were observed as early as 48 h post-irradiation (at postnatal days 2–3) and still persisted at postnatal day 21. On the other hand, X-irradiation with a single dose of 20 Gy resulted in relatively light neuronal damage and loss, while blood–brain barrier damage, astrogliosis and changes in diffusion parameters were not significantly different from those found with 40 Gy.

It is known that the volume fraction of the extracellular space in the non-irradiated cortex is large in newborn rats and diminishes with age [Lehmenkühler A. *et al.* (1993) *Neuroscience* **55**, 339–351]. X-irradiation with a single dose of 40 or 20 Gy blocked the normal pattern of volume fraction decrease during postnatal development, and in fact brought about a significant increase. At postnatal days 4–5, α increased to 0.49 ± 0.036 in layer III, 0.51 ± 0.042 in layer IV, 0.48 ± 0.02 in layer V, 0.48 ± 0.028 in layer VI and 0.48 ± 0.025 in the white matter. The large increase in α persisted three weeks after X-irradiation. Tortuosity and non-specific uptake decreased significantly at postnatal days 2–5; at days 8–9 they were not significantly different from those of control animals, while they increased significantly at days 10–21. Less pronounced but significant changes in all three diffusion parameters were also found in areas in the ipsilateral hemisphere adjacent to directly X-irradiated cortex. Compared to the control animals [Lehmenkühler A. *et al.* (1993) *Neuroscience* **55**, 339–351], a significant decrease of α, λ and k' was found in the contralateral hemisphere 48–72 h after X-irradiation. Later, α values were not significantly different from those in control animals. The decrease in λ persisted at postnatal days 4–5. A significant increase in λ and k' was found at postnatal days 18–21.

We conclude that X-irradiation of the brain in the early postnatal period, even when it results in only relatively light damage, still produces changes in all three diffusion parameters, particularly a large increase in extracellular space volume fraction in all cortical layers, and in the subcortical white matter. Such changes in extracellular volume fraction of the brain can contribute to impairment of signal transmission, e.g. by diluting ions and neuroactive substances released from cells, and can play an important role in functional deficits, as well as in the impairment of developmental processes. Moreover, the increase in tortuosity (inferred from the decrease in apparent diffusion coefficient) in the X-irradiated cortex, as well as in the contralateral hemisphere, suggests that, even when extracellular volume is large, the diffusion of the substances is substantially hindered.

Key words: cerebral cortex, diffusion analysis, extracellular space, extracellular volume, injury.

It has generally been believed that synaptic transmission is the only important signal transmission mechanism in the brain. However, chemical signaling agents such as neurotransmitters, neuropeptides, ions, trophic factors and nitric oxide, as well as metabolites, may diffuse via the extracellular space

*To whom correspondence should be addressed.

Abbreviations: BBB, blood–brain barrier; ECS, extracellular space; FCS, fetal calf serum; GFAP, glial fibrillary acidic protein; P, postnatal day; PBS, phosphate-buffered saline; TBS, Tris-buffered saline; TMA, tetramethylammonium.

(ECS) to target cells distant (micrometer to millimeter range) from the release sites. The non-synaptic transmission of substances by diffusion via the volume of the extracellular fluid has recently been termed "volume transmission".[11] This mode of communication can function between neurons as well as glial cells and may be a basis for mechanisms of information processing in functions involving large masses of cells, such as vigilance, sleep, chronic pain, hunger, depression, long-term potentiation, plastic changes and memory formation. Therefore, the ECS is an important communication pathway between cells, and the diffusion parameters of the ECS affect the movement and accumulation of substances within the ECS.

Diffusion in the ECS obeys Ficks' law, subject to two important modifications.[24,25] First, diffusion in the ECS is constrained by the restricted volume of the tissue available for diffusion particles, i.e. by the extracellular volume fraction (α). The concentration of a released substance is therefore greater than it would be in a free medium.[25] Second, the free diffusion coefficient, D, is reduced by the square of the tortuosity (λ) to an apparent diffusion coefficient $D^* = D/\lambda^2$, because a diffusing substance encounters membrane obstructions, glycoproteins and macromolecules, and therefore traverses a longer path as it diffuses between two points. Besides these two geometrical constraints, for many substances the diffusion between cells is affected by non-specific uptake, k', a factor describing the loss of material across cell membranes.[23,25] These three diffusion parameters of the ECS and their dynamic changes can be studied *in vivo* using a real-time iontophoretic method,[25] which uses ion-selective microelectrodes to follow the diffusion of an extracellular marker applied by iontophoresis (e.g. tetramethylammonium, TMA). Changes in ECS diffusion parameters (ECS volume decrease and tortuosity increase) may result from activity-related transmembrane ionic shifts and cell swelling under physiological, as well as pathophysiological, conditions.[19,26,36,42] Damage to the blood–brain barrier (BBB), cell damage, inflammation and edema formation—important factors in the manifestation of CNS diseases—could also result in an ECS volume increase and tortuosity decrease.[41,42]

Radiation therapy is an effective treatment for some human cancers. However, this therapy is limited by radiation injury. Clinical equivalents of early occurring demyelinization and necrosis include somnolence syndromes, changes in intellect, radiation myelopathies and leucoencepathies. The responses of the normal tissue immediately surrounding tumor and unavoidably irradiated areas, as well as mechanisms of radiation damage, are therefore of considerable interest. It is generally accepted[16] that radiation injury is caused by mitotic death and depletion of the various cell populations. The main syndromes of radiation injury in the CNS are very similar in rodents and humans.

The immature CNS is more sensitive to radiation than the adult nervous system, apparently due to the proliferative potential and increased radiation sensitivity of glial and/or vascular endothelial cells in the developing nervous system.[10] DNA is the molecular target for radiation-induced damage, especially in tissue which is proliferating. Besides neurotoxic effects, early postnatal X-irradiation in rats impairs gliogenesis in the spinal cord,[13,35] results in impairment of ECS K^+ and pH homeostasis,[40] and produces the breakdown of BBB, vasogenic edema and alterations in cerebral blood flow.[6,7,9,43] We might therefore expect substantial changes in ECS diffusion parameters in X-irradiated tissue.

Our recent studies revealed that in healthy animals the ECS volume fraction in the cortex, the corpus callosum and the spinal cord is large in newborn rats and diminishes with age.[20,39] Typical values of α found in animals two to three days old (P2–P3) in cortical layers III, IV, V and VI and in the corpus callosum were 0.36–0.46, while from P20 to P120 α ranged between 0.19 and 0.23. In the present study, diffusion parameters of the ECS in rat sensorimotor cortex and subcortical white matter were studied after X-irradiation at P0–P1. The diffusion parameters were studied during the first three postnatal weeks in the directly X-irradiated area, in adjacent areas of the same hemisphere and in the contralateral hemisphere. TMA diffusion profiles were analysed in control medium (agar), in individual cortical layers and in subcortical white matter (corpus callosum). Using morphological and immunohistochemical methods, the time course of the changes in diffusion parameters were compared with cell damage, BBB damage, inflammatory reaction and astrogliosis—typical signs of X-irradiation injury.

EXPERIMENTAL PROCEDURES

Preparations

Electrophysiological experiments were performed on rat pups (Wistar) from P2 to P21 anesthetized with urethane (1.6 g/kg, i.p.) and placed in a rat headholder. The body temperature was maintained at 36–37°C by supporting the rat on a heated, curved platform that enclosed the lower part of the body. The animals spontaneously breathed air. A hole, 2.5 mm in diameter, was made over the somatosensory neocortex in the hindlimb area and the dura was carefully removed. The exposed brain tissue was bathed in warmed (36–37°C) artificial cerebrospinal fluid.[25]

X-irradiation

Rat pups ($n = 63$) at P0–P1, derived from different litters, were X-irradiated. Animals were not anesthetized. While undergoing irradiation, the pups were lightly taped to a soft synthetic sponge in a box covered with a lead shield containing an aperture. A single dose of about 20 or 40 Gy was administered with an X-Ray Therapy Unit (Phillips RT 100) under the following parameters: 50 KPV, 10 mA, 10 cm FSD, total dose 20.6 or 41.1 Gy, dose rate 7.733 Gy/min, added filtration 0.3 mm aluminum, half-value layer 0.2 mm aluminum.[12,40] Before irradiation, calibration was made in a cylindrical ionization chamber. The irradiated area was restricted to the right hemiphere, to an area of the somatosensory cortex demarcated by covering the animal with

a protective lead shield 3.0 mm in thickness and containing a circular opening 3.0 mm in diameter.

All efforts were made to minimize animal suffering and to reduce the number of animals used. Experiments were performed under the inspection of the Ethical Commission of the Institute of Experimental Medicine AS CR and in accordance with the Law on Animal Protection No. 167/1993.

Histological studies

Some rats at P2–P21 were killed after electrophysiological measurements for histological and immunohistochemical studies ($n = 8$); additional animals, were also used ($n = 18$). Animals were divided into control and X-irradiated groups and perfused transcardially with saline followed by 4% paraformaldehyde in 0.1 M phosphate-buffered saline (PBS; pH 7.5). Brains were dissected and after 4 h of fixation immersed in PBS and embedded in Histosec (Merck). Serial sectioning was performed in the coronal plane. Sections 3 μm thick were mounted on silane-coated glass slides, de-paraffinized and stained. Layer II was difficult to delineate as a separate lamina during the first three postnatal days, because migration of neurons into these layers still occurs during this period (for details see Lehmenkühler *et al.*[20]). Measurements in this layer, therefore, could not be performed at P0–P3.

In situ *tailing*. *In situ* tailing was used to identify DNA fragmentation as described by Gold *et al.*[14,15] Brain sections were predigested by proteinase K in Tris-buffered saline (TBS) for 15 min at 37°C. After proteinase treatment and washing in TBS, sections were dehydrated in a series of alcohols, fixed in chloroform for 20 s and then rehydrated in the alcohol series to the TBS. For *in situ* tailing, sections were incubated for 1 h in a mixture of digoxigenin-labeled nucleotides, $CoCl_2$ and terminal transferase in TBS. Sections were then washed in TBS and unspecific antibody binding was blocked by 10% fetal calf serum (FCS) for 10 min. Sections were then incubated in alkaline phosphatase-labeled anti-digoxigenin antibody diluted in TBS with 10% FCS. The immune complex was visualized by alkaline phosphatase substrate (levamisol, dimethylformamide, naphthol-ASMX-phosphate, Tris, pH 8.2) and Fast Blue salt (Sigma). Nuclear Fast Red was used for counterstaining. Sections were covered with an oil–gelatin mixture.

Immunohistochemistry. The BBB leakage, infiltration by macrophages and T-lymphocytes, astrogliosis and the presence of fibronectin in extracellular space were identified using specific antibodies: anti-rat albumin, anti-rat immunoglobulin, ED1, W3/13, anti-glial fibrillary acidic protein (GFAP) and anti-fibronectin. De-paraffinized sections were transferred to PBS, incubated for 10 min in 10% FCS and then incubated with primary antibodies. All primary antibodies were diluted in 10% FCS and 3% rat serum in PBS. Endogenous peroxidase was blocked with 0.2% H_2O_2 in methanol for 30 min. After washing in PBS, sections were incubated for 1 h with biotinylated secondary antibodies diluted in 10% FCS and 3% rat serum in PBS, then washed and incubated for 1 h in avidin peroxidase (Sigma) diluted 1:70. The immune complex was visualized using 3,3′-diaminobenzidine tetrachloride (Sigma) and H_2O_2. Sections were counterstained with hematoxylin and covered with acrylic mounting medium (Solacryl, Sanitas, CR).

Measurements of extracellular space diffusion parameters

Ion-selective microelectrodes were used to measure TMA diffusion parameters in the ECS. Ion-selective microelectrodes for TMA were made from double-barreled theta glass tubing (Kuglstatter, Garching, Germany) as described

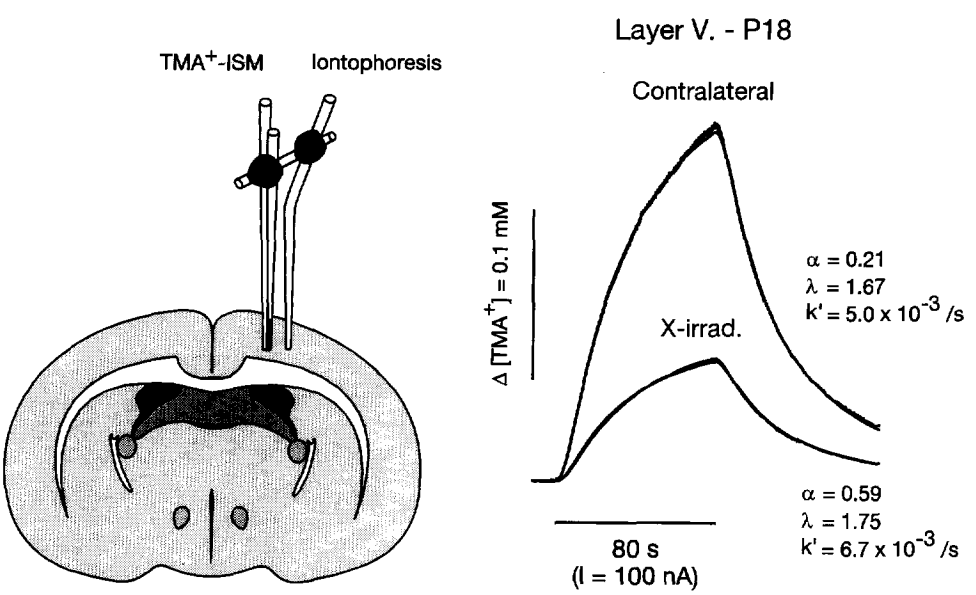

Fig. 1. Experimental set-up and TMA diffusion curves. Left: schema of the experimental arrangement. TMA selective double barreled ion-selective microelectrode (ISM) was glued to a bent iontophoresis microelectrode. The separation between electrode tips was 130–200 μm. Right: typical records obtained with this set-up in cortex of animal at P18. In this figure, as well as in Fig. 10, the concentration scale is linear and the theoretical diffusion curve [equation (1)] is superimposed on each data curve. When the electrode array was inserted into lamina V of the cortex and the iontophoretic main current applied, the resulting increase in concentration was much smaller in the X-irradiated hemisphere than that in the contralateral hemisphere, apparently due to larger volume fraction. The separation between the ion-selective microelectrode and iontophoresis electrode tips was 186 μm. The values of α, λ and k' are shown with each record. Both recordings were made in the same animal using the one-microelectrode array. Electrode transport number $n = 0.304$.

Table 1. Severity and time course of morphological and immunohistochemical changes in X-irradiated brain after a single dose of 40 or 20 Gy administered at P0–P1

Age (days)	Hematoxylin–eosin condensed at pycnotic nuclei *In situ* tailing DNA fragmentation		Neuronal loss		Immunoglobulin G or albumin leakage BBB damage		ED1 activated macrophages and microglia		GFAP astrogliosis		Fibronectin	
	20 Gy	40 Gy	20 Gy	40 Gy	20 Gy	40 Gy	20 Gy	40 Gy	20 Gy	40 Gy	20 Gy	40 Gy
2–3	+ +	+ + +	+	+ +	0	0	+	+	+	+	—	+
4–5	+ +	+	+	+ +	+	+	+	+	+ +	+ +	—	+
8–9	0	+	+	+ + +	+ +	+ + +	+	+ + +	+ + +	+ + +	—	+ +
10–11	0	+	+	+ + +	+ +	+ + +	0	+ +	+ + +	+ + +	—	+ + +
18–21	—	0	—	+ +	—	+ +	—	+	—	+ + +	—	+ +

The changes followed in animals at P2–P21. + + +, maximal and severe changes; + +, medium changes; +, minimal and mild changes; 0, no change with respect to control animals; —, not studied.

elsewhere.[20] The ion exchanger was Corning 477317 and the ion-sensing barrel was back-filled with 100 mM TMA chloride, while the reference barrel contained 150 mM NaCl. Electrodes were calibrated using the fixed-interference method before and after each experiment in a sequence of solutions of 150 mM NaCl + 3 mM KCl with the addition of the following concentrations of TMA chloride (mM): 0.0003, 0.001, 0.003, 0.01, 0.03, 0.1, 0.3, 1.0, 3.0, 10.0. Calibration data were fitted to the Nikolsky equation to determine electrode slope and interference.[27]

For TMA diffusion measurements, iontophoresis pipettes were prepared from theta glass. The shank was bent, before back-filling with 1 M TMA chloride, so that it could be aligned parallel to that of the ion-selective microelectrode. Electrode arrays were made by gluing together an iontophoresis pipette and a TMA ion-selective microelectrode with a tip separation of 130–200 μm (Fig. 1). Typical iontophoresis parameters were +20 nA bias current (continuously applied to maintain a constant transport number), with +100 nA current steps of 80 s duration to generate the diffusion curve.

Potentials recorded on the reference barrel of the ion-selective microelectrode were subtracted from the ion-selective barrel voltage measurements by means of buffer and subtraction amplifiers. TMA diffusion curves were captured on a digital oscilloscope (Nicolet 3091) and then transferred to a PC-compatible, 486 computer, where they were analysed by fitting the data to a solution of the diffusion equation (see below) using the program VOLTORO (Nicholson C., unpublished).

TMA concentration–time curves were first recorded in 0.3% agar (Difco, Special Noble Agar) dissolved in 150 mM NaCl, 3 mM KCl and 0.3 mM TMA in a Lucite cup that could be placed just above the brain. The array of electrodes was then lowered into the cortex to depths coinciding with the known distribution of the layers at the various ages used.[20]

The diffusion curves obtained from the various layers of the cortex were analysed to yield α and λ and the non-specific, concentration-dependent uptake term, k' (s^{-1}). These three parameters were extracted by a non-linear curve fitting simplex algorithm operating on the diffusion curve described by equation (1), which represents the behavior of TMA, assuming that it spreads out with spherical symmetry, when the iontophoresis current is applied for duration S. In this expression, C is the concentration of the ion at time t and distance r. The equation governing the diffusion in brain tissue is:

$$C = G(t) \quad t < S \text{ for the rising phase of the curve}$$

$$C = G(t) - G(t - S) \quad t > S \text{ for the falling phase of the curve.}$$

The function $G(u)$ is evaluated by substituting t or $t - S$ for u in the following equation.[23]

$$G(u) = (Q\lambda^2/8\pi D\alpha r)\{\exp[r\lambda(k'/D)^{1/2}]\operatorname{erfc}[r\lambda/2(Du)^{1/2} + (k'u)^{1/2}] + \exp[-r\lambda(k'/D)^{1/2}]\operatorname{erfc}[r\lambda/2(Du)^{1/2} - (k'u)^{1/2}]\}. \quad (1)$$

The quantity of TMA delivered to the tissue per second is $Q = In/zF$, where I is the step increase in current applied to the ionotophoresis electrode, n is the transport number, z is the number of charges associated with substance iontophoresed (+1 here) and F is Faraday's electrochemical equivalent. The function "erfc" is the complementary error function. When the experimental medium is agar, by definition, $\alpha = 1 = \lambda$ and $k' = 0$, and the parameters n and D are extracted by the curve fitting. Knowing n and D, the parameters α, λ and k' can be obtained when the experiment is repeated in the brain.

Statistical analysis

Results of the experiments were expressed as the mean ± S.E.M. Statistical analysis of the differences between groups was evaluated by one-way ANOVA. Values of $P < 0.05$ were considered significant.

RESULTS

Morphological and immunohistochemical changes in X-irradiated brain

Histological and immunohistochemical changes were studied between P2 and P21 after X-irradiation with a single dose of 40 Gy at P0–P1. Already at

Fig. 2. Coronal sections of the animals with X-irradiated right hemisphere. (a) A diagrammatic representation of indicated areas. (b) *In situ* tailing shows DNA fragmentation in apoptotic nuclei in an animal at P3 (× 190). (c) Coronal section of whole brain at P3 after *in situ* tailing (× 18). (d) BBB damage revealed by immunoglobulin G leakage in X-irradiated hemisphere in an animal at P7 (× 15). (e) Higher magnification of the X-irradiated regions showing immunoglobulin G in cytoplasm of damaged cells (× 140).

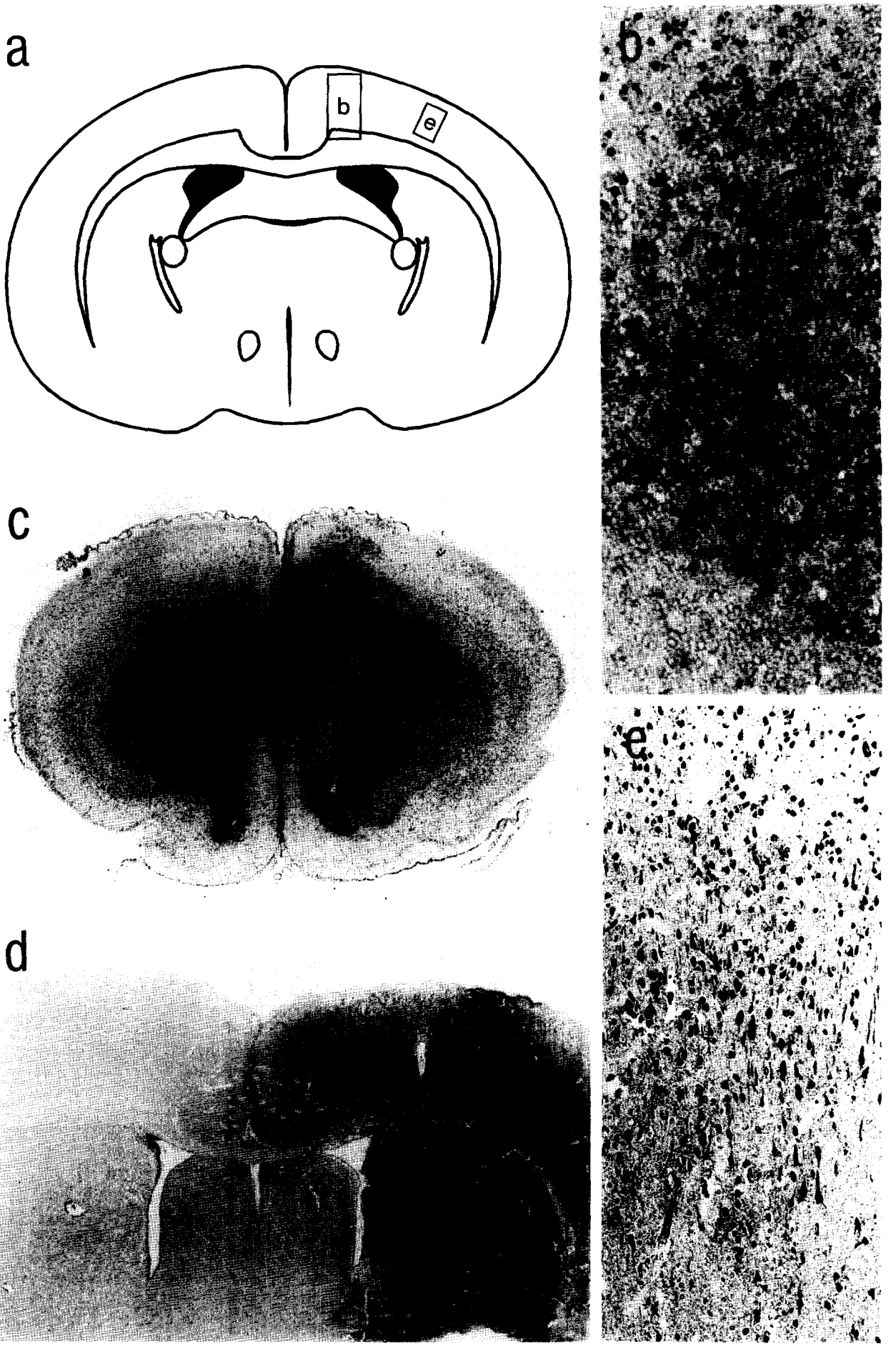
a
b
e
b
c
d
e

P2–P3, hematoxylin–eosin staining showed many damaged cells, both neurons and glia, with condensed, pycnotic nuclei, resembling the characteristic features of apoptosis. At P2–P3, *in situ* tailing showed DNA fragmentation within the apoptotic nuclei (Table 1). Damage was most severe in the periventricular matrix zone in both hemispheres (Fig. 2b, c). Dying cells in the periventricular matrix zone formed clusters between normal cells. In X-irradiated cortex, the damage was more severe in laminae V and VI, while there were fewer damaged cells in laminae II–IV.

Clearly, fewer damaged cells were found after X-irradiation with 20 Gy (Table 1) and only a few apoptotic cells were found in areas about 2 mm away from the edge of the lesion, as during normal development. While in later stages incomplete parenchymal necrosis was found after X-irradiation with 40 Gy, rather mild loss of neurons was found with 20 Gy and almost no loss was observed in non-irradiated parts of the cortex and in the contralateral hemisphere.

Immunoglobulin G and albumin leakage as a marker of BBB damage was studied from P2 to P21. In control animals, only minor staining of the meninges was found. In X-irradiated animals (40 or 20 Gy), no BBB leakage was found at P2–P3, and discrete immunoglobulin G and albumin extravasation was found at P4–P5, while strong protein leakage was present at P7–P8. The extensive leakage through the whole X-irradiated hemisphere persisted at P10–P11 (Fig. 2d), while it decreased slightly at P17–P21 (Table 1). It is therefore evident that severe BBB damage occurred at P7–P8 after X-irradiation with both 40 and 20 Gy. Immunoglobulin G and albumin were also sometimes found in the cytoplasm of damaged cells (Fig. 2e).

Activated macrophages and microglial cells were identified using ED1 antibodies. At P3, only subcortical layers were infiltrated with macrophages after X-irradiation, while no infiltration was seen in the cortex (Fig. 3a, b). A discrete infiltration occurred at P4–P5; however, at P7–P8, cortical lesions were full of ED1-stained cells (Fig. 3c, d). At P10–P11, the number of ED1-positive cells decreased, and only a few stained cells were found in the lesion at P17–P18 (Table 1). In less damaged cortex after X-irradiation with 20 Gy, only slight infiltration by macrophages was found, suggesting mild damage. In control animals, T-lymphocytes identified with W3/13 antibodies were seldom found in the meninges and ventricles. In X-irradiated animals, the number of T-lymphocytes was not significantly increased at P2–P21.

In control animals, GFAP staining in the cortex, as well as in subcortical white matter, gradually increased with postnatal development. At P18–P21, the cortex and corpus callosum were diffusely stained with GFAP, with many astrocytes attached to the blood vessels. In animals X-irradiated with either 20 or 40 Gy, GFAP staining revealed astrocyte proliferation and hypertrophy. Astrocytes had thick, densely stained processes (Fig. 4d). GFAP staining had already increased at P2–P3. Figure 4a and b shows invasion of reactive astrocytes into the X-irradiated hemisphere and, to a lesser degree, the contralateral hemisphere. Astrogliosis was maximum at P8–P11 (Fig. 4d) and persisted at P18–P21 (Table 1), suggesting the formation of a gliotic scar. At P8–P21, an increase in GFAP staining was also found in the contralateral and non-irradiated parts of the ipsilateral hemisphere, but it was much less pronounced than in X-irradiated regions (Fig. 4c, d).

Staining with antibodies against fibronectin in control animals showed only light diffuse staining from P3 to P11; this staining disappeared in animals at P18. In the X-irradiated hemisphere, an increase of fibronectin expression was found in all lesioned cortical layers at P8–P21 (Table 1, Fig. 5) and in the subcortical white matter. There was no increase in fibronectin staining in the contralateral hemisphere.

Diffusion parameters in gray and white matter

The extracellular space volume fraction, tortuosity and non-specific uptake in the normally developing rat cortex and subcortical white matter have been studied in detail by Lehmenkühler *et al.*[20] The volume fraction is large in newborn rats and diminishes with age. A substantial decrease of the ECS volume fraction in gray matter was observed at P8–P9. The "adult" (P90–P120) values of all three ECS diffusion parameters were reached in gray matter at P10–P11 and in white matter at P20–P21, apparently due to extensive gliogenesis and myelination.[20] In these experiments, we studied the diffusion parameters α, λ and k' in cortical layers III, IV, V and VI and in subcortical white matter, including the corpus callosum, of rats at P2–P3, P4–P5, P10–P11 and P18–P21, which had received a single 20 or 40 Gy dose of X-irradiation at P0–P1. The diffusion parameters in both the X-irradiated (Table 2) and contralateral hemisphere (Table 3) were compared with those of non-irradiated, control animals which were taken from the same litters (for the control values see Table 1 in Lehmenkühler *et al.*[20]).

At P2–P3, i.e. 24–48 h after X-irradiation, there was no significant decrease in α in gray or white matter in the X-irradiated hemisphere (Table 2). However, λ decreased significantly in laminae V and VI and in the white matter, and k' decreased significantly in laminae IV, V and VI (Table 2). Moreover, the values of α, λ and k' also decreased significantly in the contralateral hemisphere, α and λ in laminae V and VI and the white matter, and k' in laminae IV, V and VI and the white matter (Table 3).

At P4–P5, α increased significantly in all cortical layers as well as in the white matter of the X-irradiated hemisphere (Table 2), while in the contralateral cortex and white matter, α was not significantly different from the control values measured

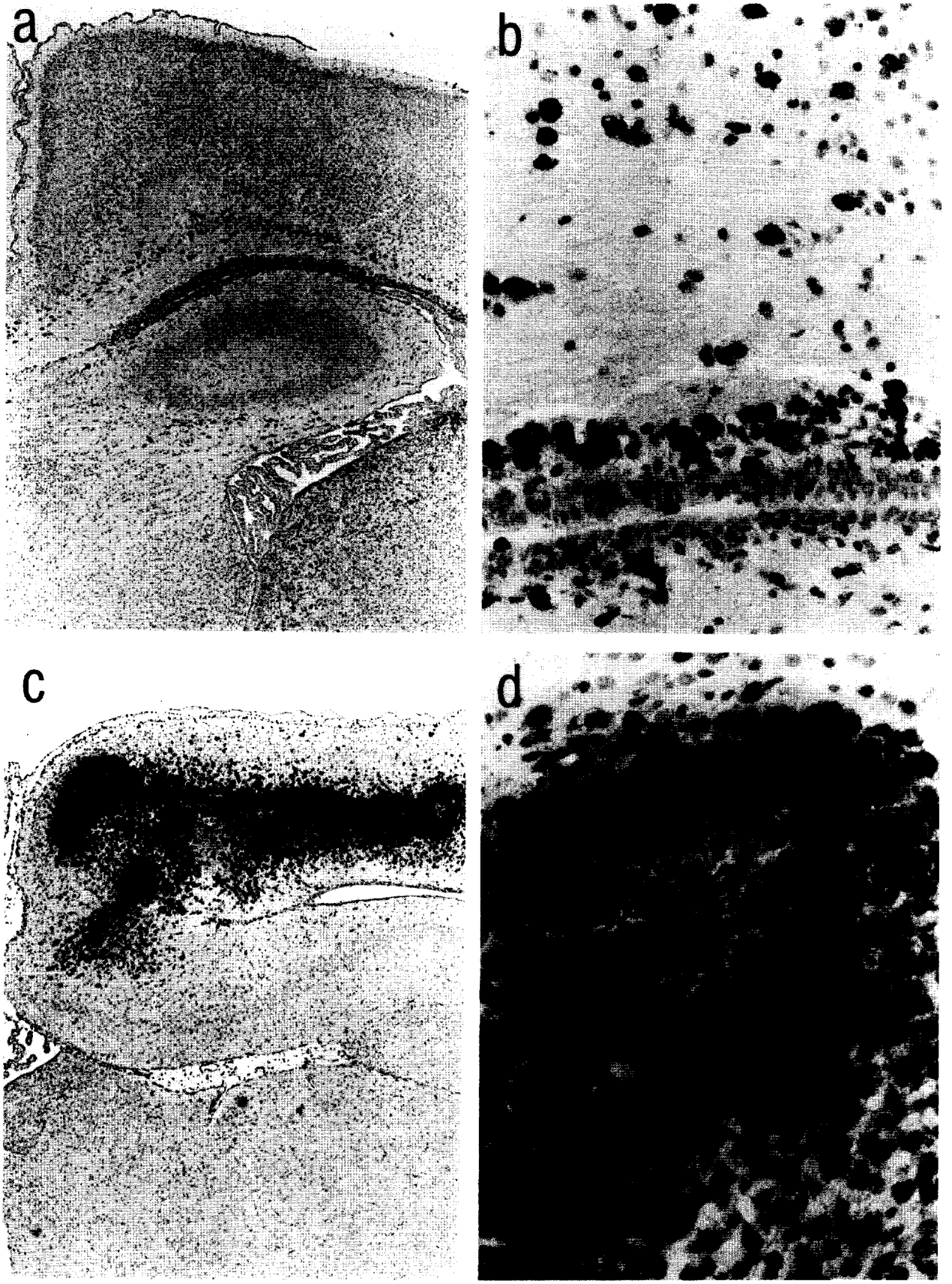

Fig. 3. Coronal section of the X-irradiated hemisphere stained with ED1 antibodies. Overview of the X-irradiated cortex and subcortical regions in animal at P3 (a) and P8 (c). At P3 only subcortical layers were infiltrated by macrophages, while at P8 the cortical lesion was full of ED1-stained cells. (b, d) Higher magnification of the lesion at P3 (b) and P8 (d). (a) ×70; (c) ×45; (b, d) ×400.

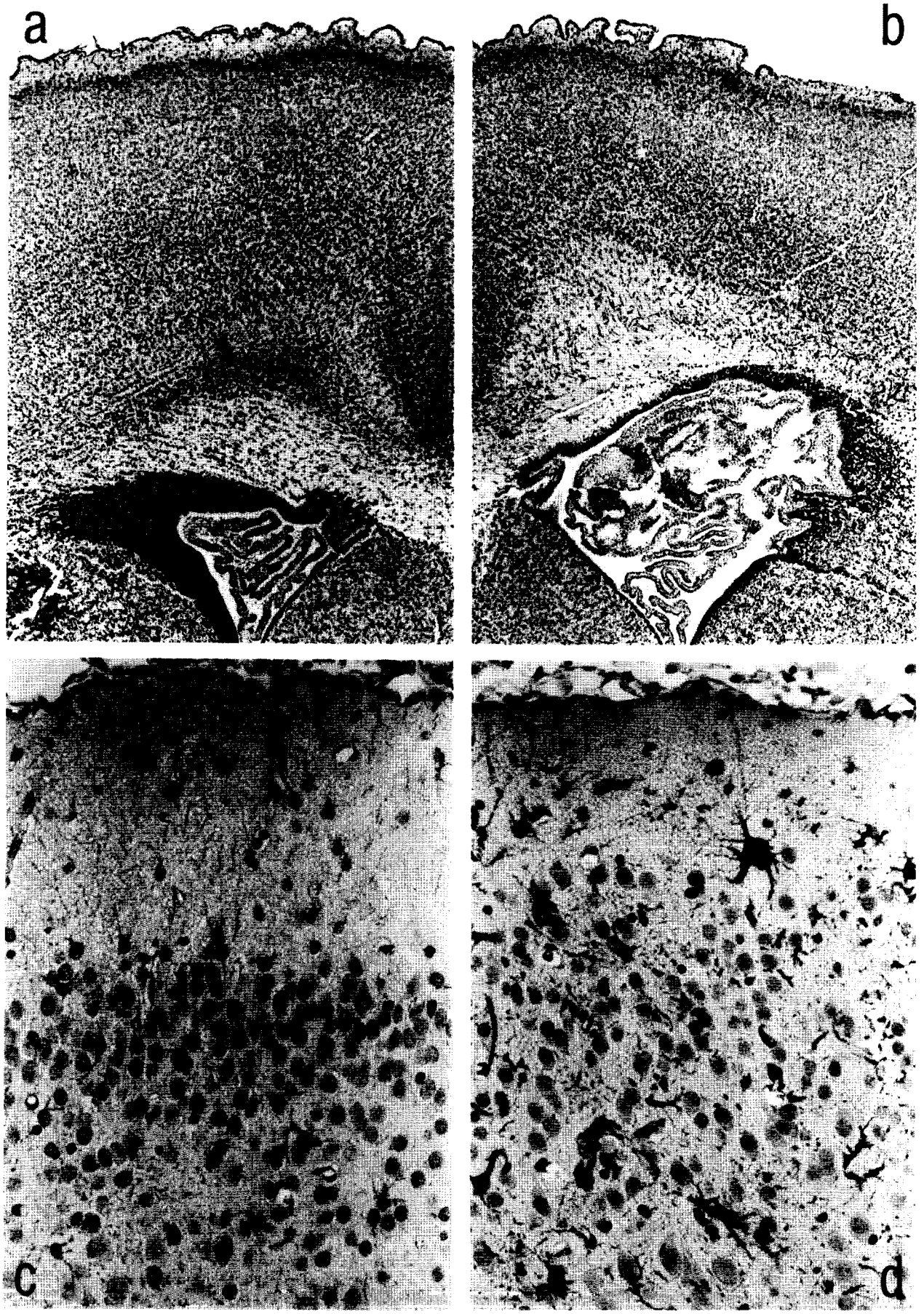

Fig. 4.

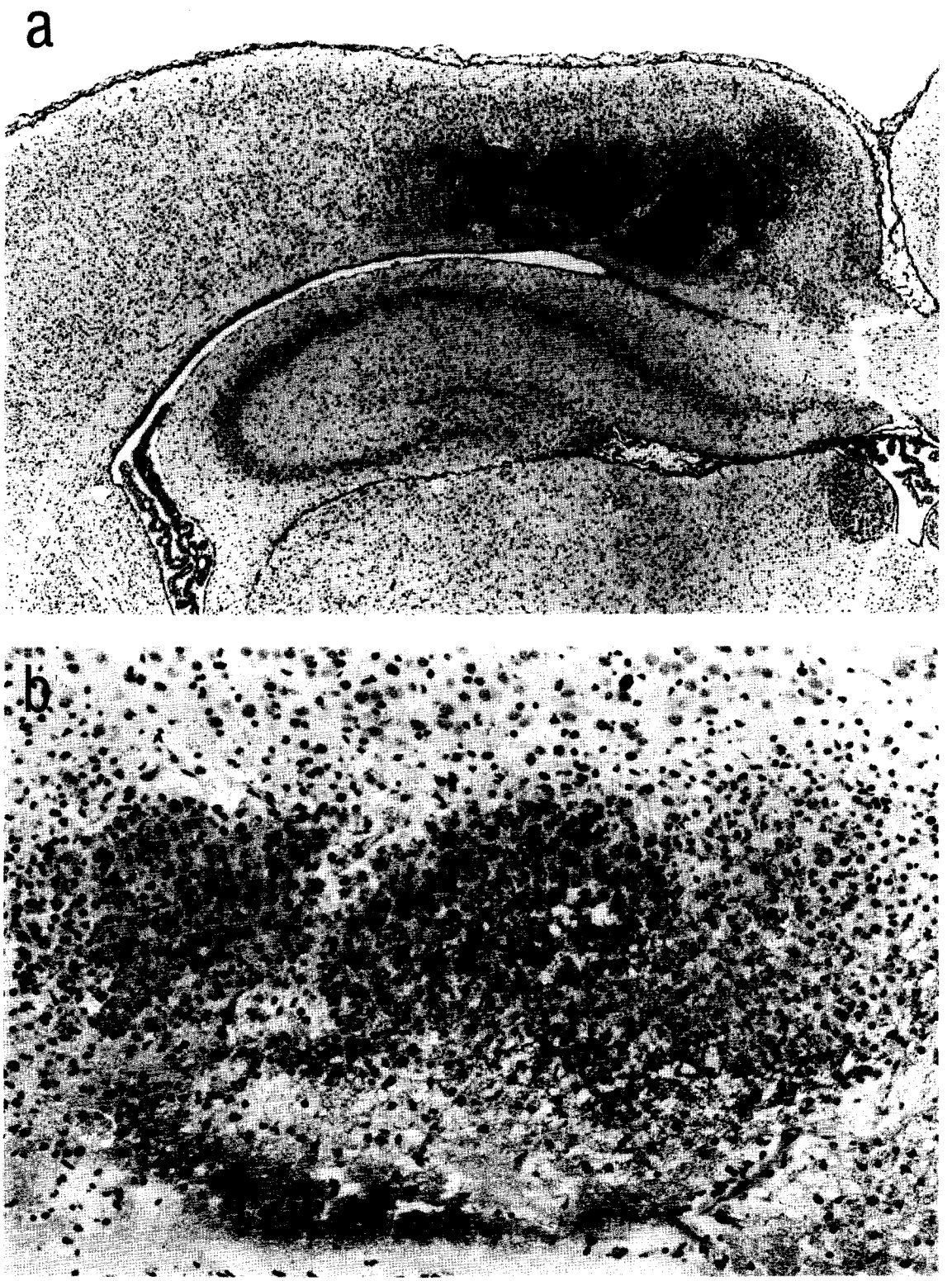

Fig. 5. (a) Coronal section of the X-irradiated hemisphere of the animal at P8 shows the cortical lesion immunostained with anti-fibronectin (× 40). (b) Higher magnification of the cortical lesion densely stained with anti-fibronectin (× 200).

Fig. 4. Astrogliosis in X-irradiated cortex and subcortical white matter. (a, b) Coronal section of the left and right (X-irradiated) hemispheres in an animal at P3 immunostained with anti-GFAP. Note the greater invasion of the X-irradiated hemisphere (b) by reactive astrocytes (× 40). (c, d) Higher magnification of the cortex at P11 reveals many fewer GFAP-positive cells in the contralateral hemisphere (c) than in the X-irradiated hemisphere (d) (× 400).

Table 2. Extracellular space diffusion parameters in X-irradiated animals as a function of age in postnatal days and cortical layers or subcortical white matter

Age (days)	Cortical layer III	IV	V	VI	White matter
40 Gy					
2–3	No data available	$\alpha = 0.40 \pm 0.03$ $\lambda = 1.59 \pm 0.02$ $k' = 1.3 \pm 0.8 \times 10^{-3}$/s† $n = 3$	$\alpha = 0.38 \pm 0.02$ $\lambda = 1.53 \pm 0.04$† $k' = 1.0 \pm 0.3 \times 10^{-3}$/s† $n = 3$	$\alpha = 0.38 \pm 0.038$ $\lambda = 1.40 \pm 0.024$† $k' = 3.0 \pm 0.7 \times 10^{-3}$/s† $n = 4$	$\alpha = 0.47 \pm 0.034$ $\lambda = 1.43 \pm 0.027$† $k' = 5.2 \pm 0.8 \times 10^{-3}$/s $n = 6$
4–5	$\alpha = 0.49 \pm 0.036$* $\lambda = 1.56 \pm 0.029$ $k' = 2.8 \pm 0.7 \times 10^{-3}$/s $n = 11$	$\alpha = 0.51 \pm 0.042$* $\lambda = 1.55 \pm 0.029$ $k' = 2.3 \pm 0.7 \times 10^{-3}$/s $n = 9$	$\alpha = 0.48 \pm 0.02$* $\lambda = 1.49 \pm 0.021$† $k' = 2.6 \pm 0.7 \times 10^{-3}$/s† $n = 16$	$\alpha = 0.48 \pm 0.028$* $\lambda = 1.42 \pm 0.02$† $k' = 2.7 \pm 0.5 \times 10^{-3}$/s $n = 15$	$\alpha = 0.48 \pm 0.025$* $\lambda = 1.38 \pm 0.027$† $k' = 3.7 \pm 1.1 \times 10^{-3}$/s $n = 8$
8–9	$\alpha = 0.50 \pm 0.032$* $\lambda = 1.63 \pm 0.03$ $k' = 2.5 \pm 0.8 \times 10^{-3}$/s $n = 9$	$\alpha = 0.46 \pm 0.039$* $\lambda = 1.60 \pm 0.033$ $k' = 3.7 \pm 1.2 \times 10^{-3}$/s $n = 6$	$\alpha = 0.47 \pm 0.038$* $\lambda = 1.58 \pm 0.027$ $k' = 4.0 \pm 0.9 \times 10^{3}$/s $n = 11$	$\alpha = 0.53 \pm 0.03$* $\lambda = 1.52 \pm 0.027$ $k' = 4.0 \pm 0.8 \times 10^{-3}$/s $n = 17$	$\alpha = 0.61 \pm 0.027$* $\lambda = 1.45 \pm 0.026$† $k' = 4.6 \pm 0.5 \times 10^{-3}$/s $n = 9$
10–11	$\alpha = 0.37 \pm 0.017$* $\lambda = 1.57 \pm 0.024$ $k' = 4.8 \pm 1.2 \times 10^{-3}$/s $n = 6$	$\alpha = 0.35 \pm 0.026$* $\lambda = 1.68 \pm 0.035$* $k' = 4.3 \pm 0.8 \times 10^{-3}$/s $n = 6$	$\alpha = 0.34 \pm 0.017$* $\lambda = 1.61 \pm 0.048$* $k' = 3.5 \pm 0.8 \times 10^{-3}$/s $n = 7$	$\alpha = 0.43 \pm 0.024$* $\lambda = 1.61 \pm 0.059$ $k' = 3.8 \pm 0.7 \times 10^{-3}$/s $n = 10$	$\alpha = 0.50 \pm 0.053$* $\lambda = 1.50 \pm 0.061$ $k' = 3.4 \pm 0.6 \times 10^{-3}$/s $n = 5$
18–21	$\alpha = 0.53 \pm 0.047$* $\lambda = 1.77 \pm 0.023$* $k' = 8.5 \pm 1.0 \times 10^{-3}$/s* $n = 5$	$\alpha = 0.49 \pm 0.06$* $\lambda = 1.79 \pm 0.015$* $k' = 8.4 \pm 1.3 \times 10^{-3}$/s* $n = 5$	$\alpha = 0.55 \pm 0.046$* $\lambda = 1.81 \pm 0.023$* $k' = 7.1 \pm 0.4 \times 10^{-3}$/s* $n = 7$	$\alpha = 0.33 \pm 0.04$* $\lambda = 1.56 \pm 0.024$* $k' = 4.9 \pm 0.5 \times 10^{-3}$/s* $n = 8$	$\alpha = 0.29 \pm 0.02$* $\lambda = 1.47 \pm 0.026$ $\lambda = 5.3 \pm 1.4 \times 10^{-3}$/s $n = 4$
20 Gy					
8–9	$\alpha = 0.52 \pm 0.038$* $\lambda = 1.66 \pm 0.032$ $k' = 3.1 \pm 0.9 \times 10^{-3}$/s $n = 7$	$\alpha = 0.48 \pm 0.043$* $\lambda = 1.60 \pm 0.033$ $k' = 3.4 \pm 1.4 \times 10^{-3}$/s $n = 5$	$\alpha = 0.49 \pm 0.051$* $\lambda = 1.60 \pm 0.035$* $k' = 3.1 \pm 1.1 \times 10^{-3}$/s $n = 8$	$\alpha = 0.44 \pm 0.023$* $\lambda = 1.55 \pm 0.034$ $k' = 4.4 \pm 1.4 \times 10^{-3}$/s $n = 8$	$\alpha = 0.60 \pm 0.032$* $\lambda = 1.48 \pm 0.019$† $k' = 4.7 \pm 0.6 \times 10^{-3}$/s $n = 7$
10–11	$\alpha = 0.31 \pm 0.013$* $\lambda = 1.60 \pm 0.017$ $k' = 4.6 \pm 1.6 \times 10^{-3}$/s $n = 10$	$\alpha = 0.34 \pm 0.028$* $\lambda = 1.60 \pm 0.042$ $k' = 3.5 \pm 0.9 \times 10^{-3}$/s $n = 9$	$\alpha = 0.30 \pm 0.007$* $\lambda = 1.62 \pm 0.059$* $k' = 2.0 \pm 0.5 \times 10^{-3}$/s† $n = 10$	$\alpha = 0.38 \pm 0.019$* $\lambda = 1.65 \pm 0.063$* $k' = 3.7 \pm 0.9 \times 10^{-3}$/s $n = 11$	$\alpha = 0.45 \pm 0.027$* $\lambda = 1.54 \pm 0.061$ $k' = 3.5 \pm 0.7 \times 10^{-3}$/s $n = 12$

α is ECS volume fraction, λ is ECS tortuosity, k' is non-specific cellular uptake, and n is number of experiments. Statistical analysis of the differences between groups was evaluated by one-way ANOVA. Significant differences ($P < 0.05$) were calculated with respect to control (naive) animals from the same litters (for control values see Table 1 in Lehmenkühler *et al.*[20]) and are marked by an asterisk (significant increase) or dagger (significant decrease).

Table 3. Extracellular space diffusion parameters in brain hemisphere contralateral to X-irradiation as a function of age in postnatal days and cortical layers or subcortical white matter

Age (days)	Cortical layer III	IV	V	VI	White matter
40 Gy					
2–3	No data available	$\alpha = 0.32 \pm 0.024$ $\lambda = 1.49 \pm 0.054$ $k' = 1.8 \pm 0.9 \times 10^{-3}$/s† $n = 5$	$\alpha = 0.29 \pm 0.018$† $\lambda = 1.43 \pm 0.04$† $k' = 2.5 \pm 0.4 \times 10^{-3}$/s† $n = 8$	$\alpha = 0.34 \pm 0.014$† $\lambda = 1.34 \pm 0.03$† $k' = 2.2 \pm 0.6 \times 10^{-3}$/s† $n = 9$	$\alpha = 0.40 \pm 0.012$† $\lambda = 1.40 \pm 0.056$† $k' = 1.8 \pm 0.4 \times 10^{-3}$/s† $n = 9$
4–5	$\alpha = 0.35 \pm 0.025$ $\lambda = 1.49 \pm 0.037$† $k' = 1.6 \pm 0.6 \times 10^{-3}$/s $n = 7$	$\alpha = 0.32 \pm 0.019$ $\lambda = 1.46 \pm 0.052$† $k' = 1.7 \pm 0.7 \times 10^{-3}$/s $n = 6$	$\alpha = 0.35 \pm 0.031$ $\lambda = 1.44 \pm 0.036$† $k' = 3.5 \pm 0.6 \times 10^{-3}$/s $n = 12$	$\alpha = 0.36 \pm 0.015$ $\lambda = 1.36 \pm 0.026$† $k' = 2.9 \pm 0.6 \times 10^{-3}$/s $n = 12$	$\alpha = 0.42 \pm 0.016$ $\lambda = 1.39 \pm 0.03$† $k' = 2.9 \pm 0.5 \times 10^{-3}$/s $n = 9$
8–9	$\alpha = 0.34 \pm 0.025$ $\lambda = 1.39 \pm 0.035$† $k' = 1.9 \pm 0.5 \times 10^{-3}$/s $n = 4$	$\alpha = 0.32 \pm 0.022$ $\lambda = 1.47 \pm 0.025$ $k' = 2.5 \pm 0.7 \times 10^{-3}$/s $n = 5$	$\alpha = 0.27 \pm 0.024$ $\lambda = 1.48 \pm 0.04$ $k' = 4.3 \pm 0.7 \times 10^{-3}$/s $n = 10$	$\alpha = 0.33 \pm 0.02$ $\lambda = 1.53 \pm 0.047$ $k' = 5.1 \pm 0.7 \times 10^{-3}$/s $n = 16$	$\alpha = 0.46 \pm 0.029$ $\lambda = 1.57 \pm 0.016$ $k' = 4.0 \pm 0.8 \times 10^{-3}$/s $n = 7$
10–11	$\alpha = 0.25 \pm 0.009$ $\lambda = 1.53 \pm 0.039$ $k' = 3.1 \pm 0.7 \times 10^{-3}$/s $n = 8$	$\alpha = 0.22 \pm 0.006$ $\lambda = 1.55 \pm 0.045$ $k' = 3.1 \pm 1.0 \times 10^{-3}$/s $n = 6$	$\alpha = 0.24 \pm 0.012$ $\lambda = 1.57 \pm 0.035$ $k' = 3.6 \pm 0.6 \times 10^{-3}$/s $n = 14$	$\alpha = 0.28 \pm 0.013$ $\lambda = 1.56 \pm 0.025$ $k' = 5.6 \pm 1.1 \times 10^{-3}$/s $n = 6$	$\alpha = 0.28 \pm 0.036$ $\lambda = 1.51 \pm 0.025$ $k' = 5.7 \pm 1.1 \times 10^{-3}$/s $n = 7$
18–21	$\alpha = 0.24 \pm 0.038$ $\lambda = 1.80 \pm 0.022$* $k' = 7.3 \pm 0.9 \times 10^{-3}$/s* $n = 12$	$\alpha = 0.24 \pm 0.013$ $\lambda = 1.74 \pm 0.012$* $k' = 5.4 \pm 0.9 \times 10^{-3}$/s $n = 5$	$\alpha = 0.23 \pm 0.01$ $\lambda = 1.75 \pm 0.033$* $k' = 6.0 \pm 0.1 \times 10^{-3}$/s $n = 4$	$\alpha = 0.23 \pm 0.01$ $\lambda = 1.52 \pm 0.04$ $k' = 4.6 \pm 0.5 \times 10^{-3}$/s* $n = 4$	$\alpha = 0.20 \pm 0.005$ $\lambda = 1.47 \pm 0.02$ $k' = 5.1 \pm 0.8 \times 10^{-3}$/s $n = 7$

For further details see footnotes to Tables 1 and 2.

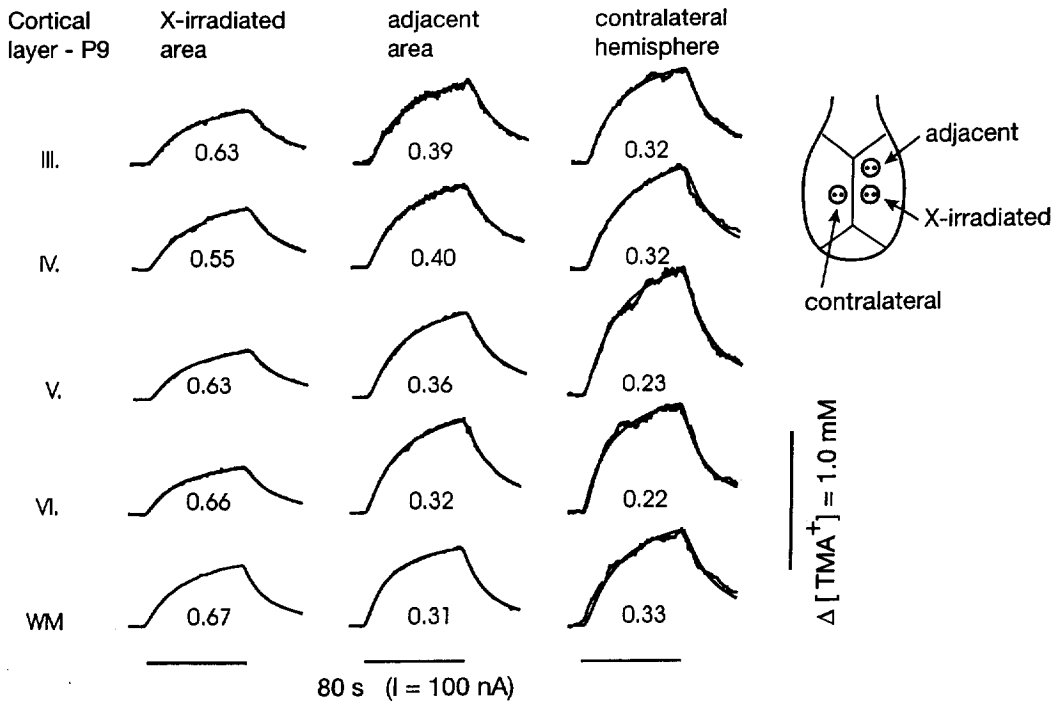

Fig. 6. Representative records obtained in cortical layers III–VI and in subcortical white matter in X-irradiated area, area adjacent to X-irradiation (2 mm rostrally from the edge of the directly X-irradiated area) and in contralateral hemisphere. For the localization of microelectrode tips, see the inset. All recordings are from the same animal at P9 and were recorded with the same microelectrode array. The values of volume fraction (α) are shown with each curve. The values of λ and k' were, from lamina III to white matter: 1.69, 1.65, 1.55, 1.60, 1.41 and 3.9×10^{-3}/s, 5.4×10^{-3}/s, 1.9×10^{-3}/s, 6.4×10^{-3}/s, 2.5×10^{-3}/s in X-irradiated area, 1.45, 1.52, 1.48, 1.48, 1.32 and 1.1×10^{-3}/s, 8.5×10^{-4}/s, 1.2×10^{-3}/s, 2.3×10^{-3}/s, 5.5×10^{-3}/s in adjacent area and 1.41, 1.53, 1.63, 1.28, 1.64 and 2.0×10^{-3}/s, 1.4×10^{-3}/s, 6.8×10^{-3}/s, 3.6×10^{-3}/s, 4.8×10^{-3}/s in contralateral hemisphere. The array spacing was 172 μm, electrode transport number $n = 0.483$.

in non-irradiated animals of the same age. In both the contralateral and X-irradiated hemisphere, λ remained significantly decreased in the gray matter as well as in the white matter, while k' was decreased only in lamina V of the X-irradiated hemisphere (Table 2).

At P8–P21, α was significantly increased in all cortical layers as well as in the white matter (Table 2). At P18–P21, the α values in X-irradiated hemisphere in layers III–V were more than twice those on the contralateral side or in non-irradiated rats (see Figs 1 and 6). No difference was found between the animals X-irradiated with 20 Gy (P8–P11) or 40 Gy. The values were even significantly larger than those for control animals at P2. Moreover, λ in the gray matter of the X-irradiated hemispheres was significantly increased from P10 to P21 and k' was increased at P18–P21. This increase in λ and k' was not observed in the white matter.

At P8–P21, the α values in the contralateral hemisphere were not significantly different from those in control animals (Fig. 6). However, at P18–P21 a significant increase in λ was found in the contralateral hemisphere in layers III, IV and V, and a significant increase in k' was found in layers III and VI (Table 3).

In addition to the dramatic changes in all three diffusion parameters in the area of direct X-irradiation and in the contralateral hemisphere, as described above, significant changes in TMA diffusion parameters were also found in areas adjacent to X-irradiated cortex and white matter of the same hemisphere. Figure 6 shows the typical TMA diffusion curves recorded in one rat (P9) in cortical layers III, IV, V and VI and in the white matter of the X-irradiated and contralateral hemisphere. Figure 6 also shows diffusion curves recorded in the same animal with the same microelectrode array in various cortical layers and in the white matter in the area adjacent to the X-irradiation (electrodes were positioned 2 mm frontally from the edge of the directly X-irradiated area in the same hemisphere). It is evident that the α values in the cortical gray matter adjacent to the X-irradiated area were lower than those in the middle of the lesion, but α was still significantly larger than that recorded in the contralateral hemisphere or in control rats.[20] No significant difference was found in the white matter below this "adjacent area" compared to the contralateral hemisphere.

We have thus found that TMA diffusion parameters for the X-irradiated cortex and corpus

callosum are changed dramatically during the first three weeks after early postnatal X-irradiation. It is evident that the changes in severely damaged brains (40 Gy) are as large as those found in relatively less damaged cortex and white matter (20 Gy). Moreover, the diffusion parameters are also changed in areas with even milder damage, i.e. in regions adjacent to X-irradiation or in the contralateral hemisphere.

DISCUSSION

Morphological and immunohistochemical changes

Experimental studies on radiation injury of the rat CNS show that relatively low doses of irradiation produce, within a few days, radiation necrosis characterized by a decrease in the number of mitotic cells[5] and a disappearance of glial precursor cells.[17,18] Some responses which occur within hours and days involve the release of various vasogenic and growth factors, while others may be based on capillary obliteration and deprivation of nutrients. It has been argued that the lesions are typically the result of infarction and edema,[4] which points to the importance of vasculature as the pathological basis. Glial cells play an important role in pathological processes, since the earliest and most predominant changes were reported in blood vessels in close association with astrocyte enlargements. BBB damage observed in monkeys 6 h to 12 days after irradiation included significant edema, along with evidence of inflammation, perivascular exudates, demyelination, gliosis and a diminished number of oligodendroglial cells.[7,10]

Our present study shows that direct irradiation of immature neurons and glia induces apoptosis. Our data show that a single 40 Gy dose of X-irradiation at P0–P1 resulted in typical radiation necrosis, while a single 20 Gy dose resulted in relatively mild damage. While apoptotic cells, massive nuclear fragmentation and astrogliosis were found as early as P2–P3, there was no change in ECS volume fraction. The cell death and astrogliosis were accompanied, however, by a decrease in tortuosity and non-specific TMA uptake. BBB damage at P4–P5, which peaked at P8–P11 (after a dose of 20 and 40 Gy), and its presence at P21 correspond well with the observed increase in ECS volume fraction at P4–P21. Even mild neuronal loss and discrete inflammatory reaction after a single dose of 20 Gy were accompanied by a significant increase in α. It is therefore apparent that the increase in α persisted in gliotic scars. The BBB damage might therefore be more important than cell loss for the increase in α. These findings correlate with the recent data obtained in our laboratory in rats with acute experimental autoimmune encephalomyelitis, characterized by demyelination, BBB damage, inflammation and astrogliosis, and also resulting in an increase in ECS volume fraction in the spinal cord.[41] Recently, ECS volume changes have been studied with the TMA method during acute cerebral inflammation following intracerebral inoculation with a weakly pathogenic strain of *Staphylococcus aureus*, but significant changes in ECS volume were not found.[21] It is also interesting that the X-irradiation-induced increase in ECS volume is "compensated" for by an increase in λ (Table 2). The massive increase of staining for fibronectin, which was found in the extracellular matrix of the X-irradiated hemisphere at P8–P21, corresponds with the observed increase in tortuosity in animals at P10–P21. The decrease in α and λ observed in the contralateral hemisphere might also be related to gliosis. The fact that gliotic reaction spreads through the necrotic lesions into the ipsilateral as well as the contralateral cortex suggests that it is induced by diffusible factors (see also Norton *et al.*[30]).

Diffusion parameters in X-irradiated cortex and subcortical white matter

To study the diffusion parameters of the X-irradiated tissue, we used the real-time iontophoretic method developed by Nicholson and Phillips.[25] The three diffusion parameters α, λ and k' were determined from concentration–time profiles of TMA, a relatively small ion with a molecular mass of 74. Its diffusion in the brain can be compared with those of biologically important ions and some neurotransmitters (e.g. acetylcholine, GABA and glutamate). The diffusion parameters of substances with greater molecular masses could be altered even more. Changes in ECS diffusion parameters can profoundly influence intercellular signal transmission and the susceptibility of the nervous tissue to damage, and could be an important factor under physiological conditions as well as in the manifestation of CNS diseases.[28,37,38] Indeed, the diffusion parameters, α, λ and k' were altered significantly during pathological states. Relative shrinkage of the ECS and increase in tortuosity as a result of cell swelling have been described for the CNS during anoxia, epileptic activity and spreading depression.[19,26,42] Recently, significantly altered diffusion parameters were found in the developing brain and spinal cord, α being almost doubled in the first postnatal week and λ typically having low values near 1.5.[20,39]

The diffusion properties of the injured nervous tissue during development have not yet been studied. In the present study, we show that diffusion properties of the ECS are changed significantly after early postnatal X-irradiation. While ECS volume fraction increases first at P4–P5, the tortuosity increases later at P10–P11. As mentioned above, the change in ECS geometry (λ is a geometrical factor) might be caused by extensive astrogliosis compensating for neuronal loss, as well as by excessive accumulation of substances in the ECS (e.g. fibronectin). During development, the diffusion parameters in different cortical layers are homogeneous, but those found in the white

matter are different.[20] By homogeneity, we mean that diffusion properties do not vary within a region. In adult animals inhomogeneity has been found in different cortical layers and in the white matter.[20] The observed differences in diffusion parameters in X-irradiated cortex therefore probably reflect different susceptibilities and/or degrees of maturation of the distinct cells in these layers. In this study we have not studied tissue anisotropy. Rice *et al.*[32] described anisotropic diffusion in the turtle cerebellum, showing that there is more than one distinct value of λ when measurements are made using different geometrical axes (x-, y- and z-axes) of the tissue. Our measurements with cortex during development (P4–P12) revealed that the diffusion in all cortical layers, as well as in the white matter, is isotropic (Syková, Škobisová and Vargová, unpublished observation).

Functional implications

The ECS constitutes the microenvironment of brain cells. Its diffusion parameters, ionic composition and the distribution of neurotransmitters, neuromodulatory compounds and metabolic substrates undergo changes during development. Moreover, the ECS is under the dynamic influence of neuronal activity. These factors can substantially affect the transmission of information in nervous tissue. The ECS is therefore an important communication channel between neurons and between neurons and glial cells, and diffusion in the ECS is an important factor in neurotransmission.[3,11,22,28,37,38]

Diffusion can be hindered under many pathological conditions, such as during anoxia[42] and chronic pain,[36] since α decreases and λ increases. On the other hand, if the volume fraction is larger and tortuosity is not substantially increased, as is the case in X-irradiated tissue in the first week after X-irradiation, substances diffusing through the ECS to target structures may not reach effective concentrations to act at particular receptors. However, in the second and third weeks the increase in tortuosity, inferred from the decrease in the apparent diffusion coefficient in the X-irradiated cortex as well as in the contralateral hemisphere, suggests that even when the extracellular volume is large, the diffusion of the substances is substantially hindered. The tortuosity increase observed in the contralateral hemisphere was not accompanied by changes in volume fraction. This suggests that changes in the geometry of the ECS and in the apparent diffusion coefficient may, under pathological conditions, occur independently of α. Important events affected by altered diffusion parameters involve the extrasynaptic movement of classical transmitters such as dopamine, adenosine, serotonin, noradrenaline, acetylcholine and glutamate.[1,8,11,44] In addition, ECS traffic includes atypical neuromodulators such as nitric oxide, which produces its effect by diffusion,[12] although it penetrates cells as well, and other important diffusible factors like nerve growth factor. It should be kept in mind that all receptors located extrasynaptically (outside of the synaptic cleft) must be reached by the diffusion of substances through the ECS. Furthermore, externally applied drugs reach target receptors and cells only by diffusion. It is therefore of considerable interest whether large molecules, e.g. from families of neurotrophic factors, can restore function in various neurological diseases. For example, nerve growth factor prevents cell death during normal development and also preserves cells from dying in pathological conditions.[31]

Constrictions in the ECS hinder the diffusion of molecules above a critical size that lies in the range of many neurotrophic compounds. Increasing values of λ for molecules with increasing molecular weight have been recently found in rat cortical slices, indicating hindrance of the diffusion of molecules with molecular weights of 40,000 to 70,000.[29] Under pathological conditions, λ may be increased to the point of preventing movement of even smaller substances through the ECS. The situation in X-irradiated tissue two to five days post-irradiation, where α is more than double the value in normal tissue and λ is decreased, may allow the movement of larger molecules than in healthy tissue. This situation, together with the increase in BBB permeability, can be advantageous during the therapeutic application of substances. However, at about two weeks after X-irradiation (P10–P21). When λ becomes significantly increased, even the diffusion of TMA is more hindered. The diffusion properties of TMA as a relatively small ion with an apparent molecular mass of 74 can be compared with those of biologically important ions and some neurotransmitters, such as acetylcholine, GABA and glutamate. The movement of substances with greater molecular masses, such as glucose (180), ATP (500), neurohormones and neuropeptides such as dynorphin, substance P and galanin (1000–3000), and nerve growth factor (about 40,000) could therefore be more hindered than is TMA.

Radiation therapy used to retard the growth of residual brain tumors and radiation of the skull in children with leukemia frequently result in neurological and psychological complications, which range from acute, but reversible, cognitive decline to memory deficit, attention deficits, a variety of sensory, language, visuospatial, awareness and intellectual deficits and, in some cases, progressive dementia.[2,33,34] Doses of 18–35 Gy are typically administered to children, but doses above 50 Gy are also administered to patients with malignant gliomas.[16] Although in clinical practice the conventional daily fractionation is used, the total doses are comparable to those used in our experiments.

CONCLUSIONS

In our study, brain areas which received a single dose of X-irradiation (20 Gy) too low to produce

severe neuronal loss, as well as remote brain regions which either received very low doses or were indirectly affected (adjacent areas), all exhibited substantial changes in diffusion properties. The substantial alterations of the ECS volume and geometry found in our experiments therefore suggest changes in non-synaptic transmission ("volume transmission") and may contribute to the changes in brain behavior induced by radiation therapy.

Acknowledgements—The authors thank Prof. Charles Nicholson for providing us with his VOLTORO program and helpful comments. This work was supported by grant GA CR no. 309/93/1048, grant GA CR no. 309/94/1107 and by U.S.–Czech Science and Technology Program Award no. 92048.

REFERENCES

1. Agnati L. F., Fuxe K., Zoli M., Zini I., Toffano G. and Ferraguti F. (1986) A correlation analysis of the regional distribution of central enkephaline and beta-endorphin immunoreactive terminals and of opiate receptors in adult and old male rats. Evidence for the existence of two main types of communication in the central nervous system: the volume transmission and the wiring transmission. *Acta physiol. scand.* **128,** 201–207.
2. Armstrong C., Mollman J., Corn B. W., Alavi J. and Grossman M. (1993) Effects of radiation therapy on adult brain behavior: evidence for a rebound phenomenon in a phase 1 trial. *Neurology* **43,** 1961–1965.
3. Bach-y-Rita P. (1993) Neurotransmission in the brain by diffusion through the extracellular fluid: a review. *NeuroReport* **4,** 343–350.
4. Blakemore W. F. and Palmer A. C. (1982) Delayed infarction of spinal cord white matter following X-irradiation. *J. Path.* **137,** 273–280.
5. Cavanagh J. B. and Hopewell J. W. (1972) Mitotic activity in the subependymal plate of rats and the long-term consequences of X-irradiation. *J. neurol. Sci.* **15,** 471–482.
6. Cavennes W. F., Tanaka A., Hess K. H., Kemper T. L., Tso M. O. and Zimmerman L. (1974) Delayed brain swelling and functional derangement after X-irradiation of the right visual cortex in the *Macaca mulatta*. *Radiat. Res.* **57,** 104–120.
7. Clemente C. D. and Holst E. A. (1954) Pathological changes in neurons, neuroglia and blood–brain barrier induced by X-irradiation of heads of monkeys. *AMA Archs Neurol. Psychiat.* **71,** 66–79.
8. Descarries L., Séguéla P. and Watkins K. C. (1991) Nonjunctional relationships of monoamine axon terminals in the cerebral cortex of adult rat. In *Volume Transmission in the Brain. Novel Mechanisms for Neural Transmission* (eds Fuxe K. and Agnati L. F.), pp. 53–62. Raven Press, New York.
9. Fike J. R., Cann C. E., Turowski K., Higgins R. J., Chan A. S. L., Phillips T. L. and Davis R. L. (1988) Radiation dose response of normal brain. *Int. J. Radiat. Oncol. biol. Phys.* **14,** 63–70.
10. Fike J. R. and Gobbel G. T. (1991) Central nervous system radiation injury in large animal models. In *Radiation Injury to the Nervous System* (eds Gutin P. H., Leibel S. A. and Sheline G. E.), pp. 113–135. Raven Press, New York.
11. Fuxe K. and Agnati L. F. (eds) (1991) *Volume Transmission in the Brain Novel Mechanisms for Neural Transmission.* Raven Press, New York.
12. Garthwaite J. (1991) Glutamate, nitric oxide and cell–cell signaling in the nervous system. *Trends Neurosci.* **14,** 60–67.
13. Gilmore S. A. (1964) The effects of X-irradiation on the spinal cords of neonatal rats. II. Histological observations. *J. Neuropath. exp. Neurol.* **22,** 294–301.
14. Gold R., Schmied M., Giegerich G., Breitschopf H., Hartung H. P., Toyka K. V. and Lassmann H. (1994) Differentiation between cellular apoptosis and necrosis by the combined use of *in situ* tailing and nick-translation techniques. *Lab. Invest.* **71,** 219–225.
15. Gold R., Schmied M., Rothe G., Zischler H., Breitschopf H., Wekerle H. and Lassmann H. (1993) Detection of DNA fragmentation of *in situ* nick tailing translation to cell culture systems and tissue sections. *J. Histochem. Cytochem.* **41,** 1023–1030.
16. Gutin P. H., Leibel S. A. and Sheline G. E. (eds) (1991) *Radiation Injury to the Nervous System.* Raven Press, New York.
17. Hopewell J. W. (1979) Late radiation damage to the central nervous system: a radiobiological interpretation. *Neuropath. appl. Neurobiol.* **5,** 329–343.
18. Hubbard B. M. and Hopewell J. W. (1980) Quantitative changes in the cellularity of the rat subependymal plate after X-irradiation. *Cell Tiss. Kinet.* **13,** 403–413.
19. Lehmenkühler A. and Richter A. (1991) Interictal discharges: changes in size of extracellular space in relation to changes in extracellular K^+ and Na^+ concentration. *Expl Brain Res. Ser.* **20,** 23–26.
20. Lehmenkühler A., Syková E., Svoboda J., Zilles K. and Nicholson C. (1993) Extracellular space parameters in the rat neocortex and subcortical white matter during postnatal development determined by diffusion analysis. *Neuroscience* **55,** 339–351.
21. Lo W. D., Wolny A. C., Timan C., Shin D. and Hinkle G. H. (1993) Blood–brain barrier permeability and the brain extracellular space in acute cerebral inflammation. *J. neurol. Sci.* **118,** 188–193.
22. Nicholson C. (1979) Brain cell microenvironment as a communication channel. In *The Neuroscience Fourth Study Program* (eds Schmidt F. O. and Worden F. G.), pp. 457–476. MIT Press, Cambridge, MA.
23. Nicholson C. (1992) Measurement of extracellular space. In *Practical Electrophysiological Methods: A Guide for* In Vitro *Studies in Vertebrate Neurobiology* (eds Kettenmann H. and Grantyn R.), pp. 367–372. Wiley, New York.
24. Nicholson C. (1993) Ion-selective microelectrodes and diffusion measurements as tools to explore the brain cell microenvironment. *J. Neurosci. Meth.* **48,** 199–213.
25. Nicholson C. and Phillips J. M. (1981) Ion diffusion modified by tortuosity and volume fraction in the extracellular microenvironment of the rat cerebellum. *J. Physiol., Lond.* **321,** 225–257.
26. Nicholson C., Phillips J. M., Tobias C. and Kraig R. P. (1981) Extracellular potassium, calcium and volume profiles during spreading depression. In *Ion-selective Microelectrodes and Their Use in Excitable Tissues* (eds Syková E., Hník P. and Vyklický L.), pp. 211–223. Plenum Press, New York.

27. Nicholson C. and Rice M. E. (1988) Use of ion-selective microelectrodes and voltammetric microsensors to study brain cell microenvironment. In *Neuromethods: The Neuronal Microenvironment* (eds Boulton A. A., Baker G. B. and Walz W.), pp. 247–361. Humana Press, Clifton, NJ.
28. Nicholson C. and Rice M. E. (1991) Diffusion of ions and transmitters in the brain cell microenvironment. In *Volume Transmission in the Brain. Novel Mechanisms for Neural Transmission* (eds Fuxe K. and Agnati L. F.), pp. 279–294. Raven Press, New York.
29. Nicholson C. and Tao L. (1993) Hindered diffusion of high molecular weight compounds in brain extracellular microenvironment measured with integrative optical imaging. *Biophys. J.* **65,** 2277–2290.
30. Norton W. T., Aquino D. A., Hozumi I., Chiu F.-C. and Brosnan C. F. (1992) Quantitative aspects of reactive gliosis: a review. *Neurochem. Res.* **17,** 877–885.
31. Pérez-Polo R., Foreman P. J., Jackson G. R., Shan D., Taglialatela G., Thorpe L. W. and Werrbach-Perez K. (1990) Nerve growth factor and neuronal cell death. In *Molecular Neurobiology* (ed. Bazan N. G.), pp. 57–91. Human Press, New York.
32. Rice M. E., Okada Y. and Nicholson C. (1993) Anisotropic and heterogeneous diffusion in the turtle cerebellum. *J. Neurophysiol.* **70,** 2035–2044.
33. Routtenberg A. (1991) Action at a distance: the extracellular spread of chemicals in the nervous system. In *Volume Transmission in the Brain. Novel Mechanisms for Neural Transmission* (eds Fuxe K. and Agnati L. F.), pp. 295–298. Raven Press, New York.
34. Sheline G. E., Wara W. M. and Smith V. (1980) Therapeutic irradiation and brain injury. *Int. J. Radiat. Oncol. biol. Phys.* **6,** 1215–1228.
35. Sims T. J. and Gilmore S. A. (1992) Glial response to dorsal root lesion in the X-irradiated spinal cord. *Glia* **6,** 96–107.
36. Svoboda J. and Syková E. (1991) Extracellular space volume changes in the rat spinal cord produced by nerve stimulation and peripheral injury. *Brain Res.* **560,** 216–224.
37. Syková E. (1991) Activity-related ionic and volume changes in neural microenvironment. In *Volume Transmission in the Brain. Novel Mechanisms for Neural Transmission* (eds Fuxe K. and Agnati L. F.), pp. 217–336. Raven Press, New York.
38. Syková E. (1992) Ionic and volume changes in the microenvironment of nerve and receptor cells. In *Progress in Sensory Physiology* (ed. Ottoson D.), pp. 1–167. Springer, Heidelberg.
39. Syková E. and Chvátal A. (1993) Extracellular ionic and volume changes: the role in glia–neuron interaction. *J. chem. Neuroanat.* **6,** 247–260.
40. Syková E., Jendelová P., Šimonová Z. and Chvátal A. (1992) K^+ and pH homeostasis in the developing rat spinal cord is impaired by early postnatal X-irradiation. *Brain Res.* **594,** 19–30.
41. Syková E., Svoboda J. and Polák J. (1992) Extracellular space volume and tortuosity changes in the rat spinal cord evoked by afferent stimulation, anoxia and EAE. In *Abstracts of the 15th Annual Meeting of the European Neuroscience Association*, p. 3323.
42. Syková E., Svoboda J., Polák J. and Chvátal A. (1994) Extracellular volume fraction and diffusion characteristics during progressive ischemia and terminal anoxia in the spinal cord of the rat. *J. cerebr. Blood Flow Metab.* **14,** 301–311.
43. Tanaka A., Ueno H., Yamashita Y. and Cavennes W. F. (1974) Regional cerebral blood flow in delayed brain swelling following X-irradiation of the right occipital lobe in the monkey. *Brain Res.* **96,** 233–246.
44. Vizi E. S. (1984) *Non-synaptic Interactions Between Neurones: Modulation of Neurochemical Transmission.* Wiley, Chichester.

(*Accepted* 26 *June* 1995)